JETIR.ORG ISSN: 2349-5162 | ESTD Year : 2014 | Monthly Issue
JOURNAL OF EMERGING TECHNOLOGIES AND INNOVATIVE RESEARCH (JETIR)
An International Scholarly Open Access, Peer-reviewed, Refereed Journal

Analysis of Cold-Formed Steel Built-up Battened Columns Under Compression

Prof. L R Wankhade, Visharad Kende
Government College of Engineering, V.M.V Amravati, Maharashtra, India – 444604

Abstract: This paper presents a detailed numerical study of the flexural buckling strength and axial cyclic response of a cold-formed steel (CFS) channel built-up battened columns. A total 36 double channels welded back-to-back and double channel welded as face-to-face both with lip as well as for without lip batten built-up columns testing are carried out for failure with pinned ends and fixed end. A total column is divided for different slenderness ratio with respective to different channels section and their behaviour is studied. To study the effect of lip, and the effect of symmetricity of cross-section on the ultimate load carrying capacity for different slender condition. Cold-formed steel sectional dimension and properties values are taken from IS 811-1987. Geometric and material non-linearity have been included in the finite element model and the flat width to thickness ratio of all specimens are kept less than the limiting values as per IS 801-1975. Built-up batten columns are design as per IS 800-2007. Design column strength calculate by using the finite element analysis (FEA) and the axial cyclic response of a cold-formed steel batten columns are compare with each other. Also compare pin ended and fix end columns were pin end columns take lesser load due to buckle in mid-section.

Keywords: Cold-formed steel, Built-up column, Battened column, Lipped channel, Finite element analysis, Axial cyclic response, Pin end, Fix end, etc.

Introduction:

Generally, cold-formed steel construction material is different from other steel construction materials known as hot-rolled steel. Cold-formed steel products are manufactured by rolling and or pressing at room temperature. Cold-formed steel structure members may prove more economical while designing than hot-rolled members as a result of their superior strength to weight ratio and ease of construction. Light gauge cold-formed channels are commonly used as wall studs and chord members of roof trusses in steel frames housing and industrial buildings. Thin walled, cold-formed steel sections can be used efficiently as structural members of light-weight structures in cases where hot-rolled sections or others are not efficient. Cold-formed steel has several advantages such as lightness in weight, high strength and stiffness, ease of prefabrication and mass production, fast and easy erection and installation, no formwork needed, economy in transportation and handling and recyclable material etc.

The size and shape of a standard cold-formed steel member are limited because of the limitation of rolling mills. When CFS are unable to take the large load acting on the section built-up section are used. It also used when a special shape of the section is required. Also, when a large radius of gyration is required to satisfy the design requirements like slenderness ratio or λ_{v-v}. Battens are plates used to connect the main components of compression member. Battens must be placed opposite of each other while attaching on the two parallel faces of the compression member. They should be uniformly spaced thought out the length of the column. Batten are used when the compression member is loaded heavily axially. Unlike lacing member members which are included, battens are placed perpendicular to the axial of the column i.e., if compression member, say columns are vertical then battens are placed horizontally. Batten plates are placed such that the compression member is divided into a minimum of 3 bays. The battens are provided so that the strength along each axis becomes equal i.e., the radius of gyration along the y-y axis becomes equal to radius of gyration along x-x axis.

Literature Review:

Kalochairetis and Gante [1] did a numerical and analytical study on the laced built-up column to determine the collapse load and anticipated that the capacity of the member would be reduced by 50% as a result of imperfections based on research by Jayagopa and Kandasamy. Roy, et al. [2] on back-to-back battened built-up sections demonstrated how the thickness of the member and fasteners between two built-up areas affect the built-up unit’s ability to carry loads. the study's chosen specimens which were determined by AS/NZS 4600 and AISI-S100. Georgieva, et al. [4] developed the direct strength techniques methodology for Z sections joined side-by-side.

Hajirasouliha, et al. [5] highlighted the improvement in lateral strength of the arranges braced and unbraced column by 75% subjected to axial load considered during the design. In this study he suggested the best technique for constructing lipped channel sections. Dinis and Camotim [6] investigated the unique DSM method design approach was confirmed by looking into column structural behaviour against local-distortional buckling of the hat, zed, and rack-shaped sections. The connection between local-distortion buckling and failure mode in load-carrying capacity is described in the work. Hajirasouliha, and Becque [8] studied on the CFS lipped channel section and investigated both local and global flexural buckling interactions. Their ultimate load carrying capacity for the optimised lipped channel section is 19% greater than the commercially available section and was in accordance with EC 3-Part 1. Aswathy and Kumar’s [9] study on the possibility of distortional buckling increases as the specimen’s stiffness or depth of lip is reduced according to experiments on stiffened and unstiffened lipped channel sections. The study predicted that the limiting condition for distortional buckling for a partially stiffened element and provided detailed information about the distortional buckling in the stiffened lipped channel section during axial loading.

Vijayanand and Anbarasu’s [10] studies predicted that North American Specification and Euro standards are found to be unconservative by 15 to 30 %. For the purpose of preventing lateral drifting and significant lateral displacements the slenderness ratio must be limited by 75. The reason for choosing the open section rather than the closed section is based on the main findings of the research reported by Kherbouche and Megnounif [11]. Both open and closed channels joined by battened plates are used in the nonlinear finite element analysis. According to the study, the web-to-length ratio of the channels affects the stability of the column. The open parts are discovered to be conservative and local buckling affects failure. Additionally, global buckling caused the closed parts to collapse, and the results were found to be unreliable. According to Manikandan and Arun [12] the intermediate stiffeners must be used and the ratio of the length of the column to the center-to-center distance of the spacer plate will affect the torsional rigidity for the partially closed portions. It was discovered that DSM values were conservative.

Section Design:

The battened column was made from cold-formed steel equal angle section, without lip and with lipped channel sections, and hat section. All sections built-up battened column cross-section dimensions were suitably chosen. The cross-section dimensions are standard taken from IS 811-1987. The geometric properties for the six selected specimen are present in Table 1. Spacing between the chords was chosen such that moment of inertia at major axis equals to moment of inertia at minor axis. To form a batten column and ensure that built-up member acts as a unit IS 800-2007 were used. Clause no.7.7 requires that individual components of built-up compression member connector spacing be such that the effective slenderness ratio of each component does not exceed three-fourths of the slenderness ratio of the built-up member. Spacing between member is taken such that to ensure satisfy all clause given in IS code.

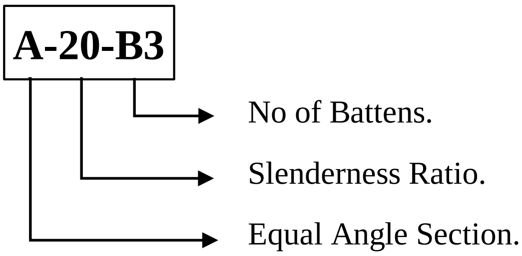

Figure 1 Labelling of Specimen

The specific names are given to specimens based on their variable geometric parameters, to save from any kind of confusion. The connection between the battens and sections is made by using weld joints. Figure 1 shows the followed naming system of a cold-formed steel built-up battened columns.

Table 1.1 Equal Angles

Naming	Slenderness Ratio	Specimen ID	Batten Width	Length (mm)	No. of battens	Max Spacing (mm)
A-20-B3	20	50 x 50 x 2 mm @ Spacing 50 mm	78 mm	317.5	3	224
A-40-B3	40			635.6	3	446
A-60-B4	60			953.4	4	668
A-80-B4	80			1271.2	4	794
A-100-B4	100			1589	4	794
A-120-B5	120			1906.8	5	794

Table 1.2 Channels Without Lips – Rectangular

Naming	Slenderness Ratio	Specimen ID	Batten Width	Length (mm)	No. of battens	Max Spacing (mm)
C-20-B3	20	90 x 50 x 2 mm @ Spacing 38 mm	68 mm	724	3	224
C-40-B4	40			1448	4	448
C-60-B5	60			2172	5	672
C-80-B7	80			2896	7	800
C-100-B8	100			3620	8	800
C-120-B9	120			4344	9	800

Table 1.3 Channels with Lips – Rectangular

Naming	Slenderness Ration	Specimen ID	Batten Width	Length (mm)	No. of battens	Max Spacing (mm)
LC-20-B3	20	90 x 50 x 15 x 2 mm @ Spacing 26 mm	62 mm	720	3	259
LC-40-B4	40			1440	4	518
LC-60-B5	60			2160	5	777
LC-80-B7	80			2880	7	925
LC-100-B8	100			3600	8	925
LC-120-B9	120			4320	9	925

Table 1.4 Hat Section – Rectangular b > h

Naming	Slenderness Ratio	Specimen ID	Batten Width	Length (mm)	No. of battens	Max Spacing (mm)
H-20-B3	20	40 x 60 x 15 x 2 mm @ Spacing 12mm	46 mm	534	3	211
H-40-B4	40			1068	4	422
H-60-B4	60			1602	4	634
H-80-B5	80			2136	5	755
H-100-B7	100			2670	7	755
H-120-B8	120			3204	8	755

Finite Element Modelling:

Finite element software ABAQUS version 2022 was used for the numerical study. Initially to analysing the post-buckling behaviour of the structure, a linear buckling analysis is performed on the specimens to obtain its buckling load and mode shape. Following this nonlinear post-buckling analysis is carried out to obtain the load versus end-shortening characteristic and to predict the ultimate load capacity. After axial cyclic response on same column is measure for load bearing capacity for varying amplitudes. Thin shell element with four nodes and six degrees of freedom at each node, S9R5 shell element, were used to model the battened columns. To choose a suitable finite element mesh for the study, convergence investigations on the column have been conducted. The element aspect ratio which is length to width is nearly equal to 1.0 for the flange and web element was used. The element measured 10×10 mm^2. Prior the end condition of column elastic lines is treated as pinned condition then after fixed condition provide for calculation of ultimate load respectively. For pinned, the applied load end condition was prevented from rotation about z-axis and translations in both x and y directions. But the unloaded end condition was prevented from translation in all three directions x, y and z directions and from rotation about z- axis. Where for fixed unloaded end condition all translation and rotation in x, y, z-axis respectively is restricted, and the load end condition remain same as pinned end. The boundary conditions were selected as an independent node which are rigid fixed MPC (Multi Point Constraint) in nature assign at the geometric centroid of the column at upper and a lower end of model. Dependent nodes are connected to the independent nodes using rigid beams and all six structural degrees of freedoms are rigidly attached to each other. This MPC acted as a rigid surface that was rigidly connected to upper and lower end of the columns as shown in Figure 2.

The specimens were loaded through the CG of the specimens in an axial direction. The mesh independent fastener option in ABAQUS was used to represent the connection between the battens and sections. The displacement control load was applied in increment to the master node using the modified RIKS method. And for axial cyclic response the model was implemented by damage initiation and damage evolution in ABAQUS. The model considers both material and geometric non-linearity. For cyclic response used measured imperfections and steel material property derives from couple tests of David A. Padilla-Llano [3]. Young's modulus of elasticity (E) and yield stress (f_y) of the steel material were considered as 201000Mpa and 250Mpa respectively taken from G Beulah Gnana Ananthi, et al. [7]. Elastic perfect plastic stress-strain curve obeying vonmises yield criterion was adopted for material modelling in the parametric study. From literature, the local as well as distortional imperfection were taken as equal to the 0.006 x w x t and 1.0 x t respectively recommended by the Schafer and Pekoz [13], in addition the global imperfection magnitude was taken as 1/1000 of the total length of batten column for nonlinear analysis at the mid- height section for both without lip and lipped channels are used for parametric study of all models to initiate the linear and nonlinear analyses.

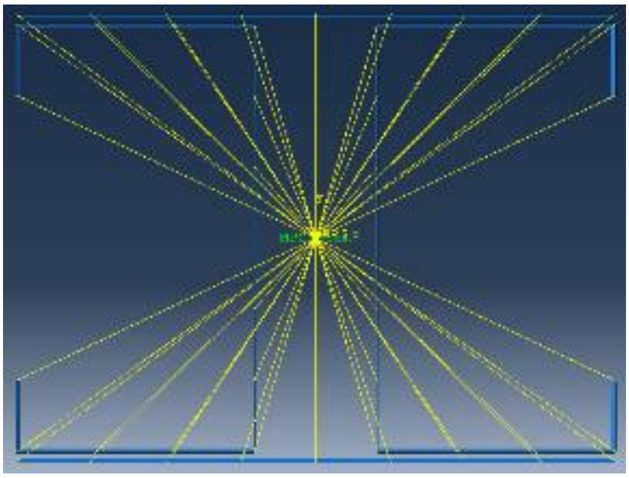

Figure 2 Parametric Model-Rigid Region

Parametric Study:

In parametric study, numerical analysis was carried out for four cross-sections as mentioned in Table 1. For without lip and lipped channel sections were assemble in both back-to-back and face-to-face fashioned. For each cross-section different member length are calculated from wide range of member slenderness ratios, varying from 20 to 120. Totally 36 number of analyses were carried out by both the methods. The ultimate strength obtained by finite element analysis is compared with the direct strength method as well as axial cyclic response for both pinned and fixed end condition as shown in Table 2.

Table 2.1 Equal Angles

Naming	Slenderness Ratio	Finite Element Analysis P_{FEA} (kN)		Axial Cyclic Response P_n (kN)		P_{FEA} / P_n	
		Pinned End	Fixed End	Pinned End	Fixed End	Pinned End	Fixed End
A-20-B3	20	232.583	301.560	239.776	307.71	0.97	0.98
A-40-B3	40	227.402	294.444	232.042	297.418	0.98	0.99
A-60-B4	60	171.680	219.003	169.980	225.776	1.01	0.97
A-80-B4	80	125.899	134.269	125.899	132.939	1.00	1.01
A-100-B4	100	86.740	101.121	82.609	109.914	1.05	0.92
A-120-B5	120	76.673	87.790	73.021	93.390	1.05	0.94
					Mean	1.01	0.96
					SD	0.03	0.03

Table 2.2.1 Back-To-Back Channels Without Lips – Rectangular

Naming	Slenderness Ratio	Finite Element Analysis P_{FEA} (kN)		Axial Cyclic Response P_n (kN)		P_{FEA} / P_n	
		Pinned End	Fixed End	Pinned End	Fixed End	Pinned End	Fixed End
BC-20-B3	20	140.855	184.928	145.211	196.731	0.97	0.94
BC-40-B4	40	150.357	193.960	181.153	215.511	0.83	0.90
BC-60-B5	60	140.010	169.012	132.084	157.955	1.06	1.07
BC-80-B7	80	125.699	150.838	118.583	139.664	1.06	1.08
BC-100-B8	100	108.962	128.306	102.794	123.371	1.06	1.04
BC-120-B9	120	89.400	103.810	81.272	92.687	1.1	1.12
					Mean	1.01	1.03
					SD	0.09	0.08

Table 2.2.2 Face-To-Face Channels Without Lips – Rectangular

Naming	Slenderness Ratio	Finite Element Analysis P_{FEA} (kN)		Axial Cyclic Response P_n (kN)		P_{FEA} / P_n	
		Pinned End	Fixed End	Pinned End	Fixed End	Pinned End	Fixed End
FC-20-B3	20	146.578	193.480	174.497	233.108	0.84	0.83
FC-40-B4	40	144.108	186.899	150.112	196.735	0.96	0.95
FC-60-B5	60	144.173	178.216	138.627	169.729	1.04	1.05
FC-80-B7	80	132.023	158.427	122.243	149.459	1.08	1.06
FC-100-B8	100	101.381	119.588	93.871	107.736	1.08	1.11
FC-120-B9	120	79.994	91.993	71.423	77.305	1.12	1.19
					Mean	1.02	1.03
					SD	0.10	0.13

Table 2.3.1 Back-To-Back Channels with Lips – Rectangular

Naming	Slenderness Ratio	Finite Element Analysis P_{FEA} (kN)		Axial Cyclic Response P_n (kN)		P_{FEA} / P_n	
		Pinned End	Fixed End	Pinned End	Fixed End	Pinned End	Fixed End
BLC-20-B3	20	192.535	255.146	196.464	271.431	0.98	0.94
BLC-40-B4	40	184.102	236.491	200.110	257.055	0.92	0.92
BLC-60-B5	60	185.507	231.883	180.103	218.757	1.03	1.06
BLC-80-B7	80	160.978	198.000	154.786	183.333	1.04	1.08
BLC-100-B8	100	146.124	173.887	140.503	159.529	1.04	1.09
BLC-120-B9	120	114.550	129.732	102.276	115.832	1.12	1.12
					Mean	1.02	1.04
					SD	0.07	0.08

Table 2.3.2 Face-To-Face Channels with Lips – Rectangular

Naming	Slenderness Ratio	Finite Element Analysis P_{FEA} (kN)		Axial Cyclic Response P_n (kN)		P_{FEA} / P_n	
		Pinned End	Fixed End	Pinned End	Fixed End	Pinned End	Fixed End
FLC-20-B3	20	205.061	271.680	220.495	292.129	0.93	0.93
FLC-40-B4	40	202.755	260.553	204.803	274.266	0.99	0.95
FLC-60-B5	60	194.150	238.687	192.227	229.506	1.01	1.04
FLC-80-B7	80	171.173	210.532	164.589	202.434	1.04	1.04
FLC-100-B8	100	140.289	164.943	128.705	154.152	1.09	1.07
FLC-120-B9	120	103.837	118.412	94.397	109.640	1.10	1.08
					Mean	1.03	1.02
					SD	0.06	0.06

Table 4 Hat Section – Rectangular b > h

Naming	Slenderness Ratio	Finite Element Analysis P_{FEA} (kN)		Axial Cyclic Response P_n (kN)		P_{FEA} / P_n	
		Pinned End	Fixed End	Pinned End	Fixed End	Pinned End	Fixed End
H-20-B3	20	246.372	322.740	267.795	332.721	0.92	0.97
H-40-B4	40	248.323	315.370	264.173	325.123	0.94	0.97

H-60-B4	60	231.215	283.643	228.925	281.113	1.01	1.01
H-80-B5	80	188.698	232.098	181.440	221.045	1.04	1.05
H-100-B7	100	132.659	157.864	119.512	139.702	1.11	1.13
H-120-B8	120	96.452	111.919	86.117	97.320	1.12	1.15
					Mean	1.02	1.05
					SD	0.08	0.07

As a sample, the deformation shape at failure load from finite element method and axial cyclic response is shown in Figure 3. Figure 4 shows the load vs axial shortening curve comparison for slenderness ratio 80 of batten column. And Figure 5 shows curve of monotonic and cyclic load on specimen A-20-B3.

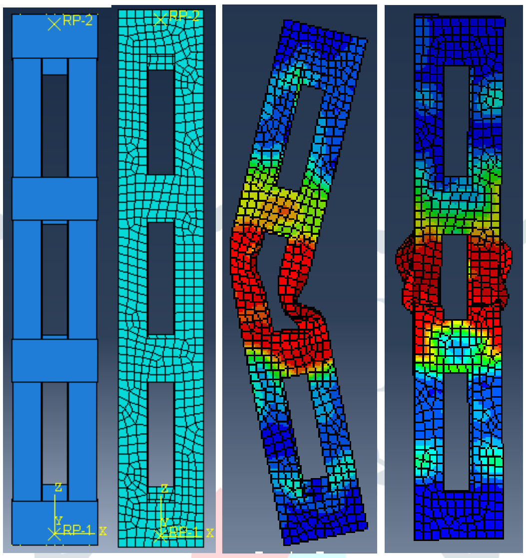

Figure 3 Deformed shape at failure of specimen A-60-B4

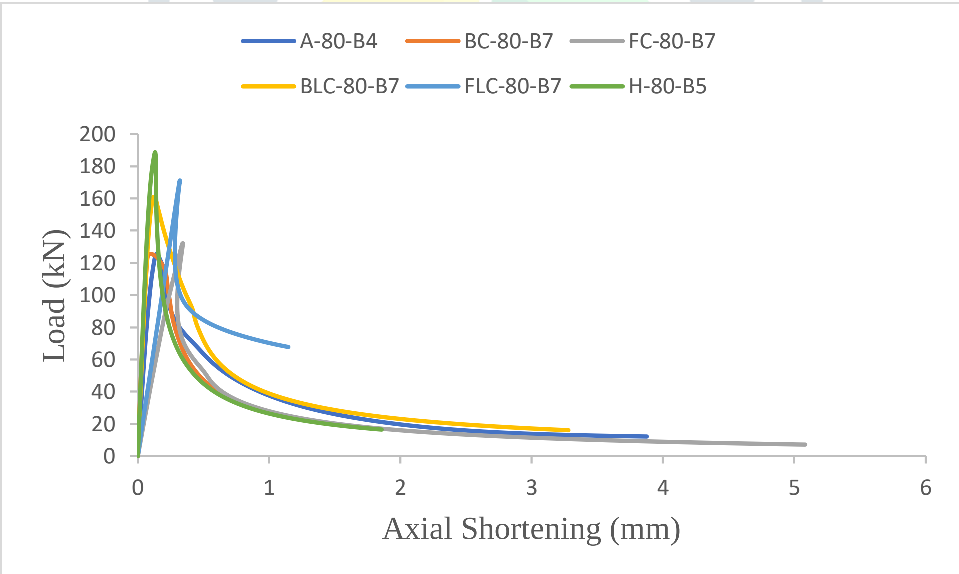

Figure 4 Axial Shortening Behaviour Comparison of Sections for Slenderness Ratio 80.

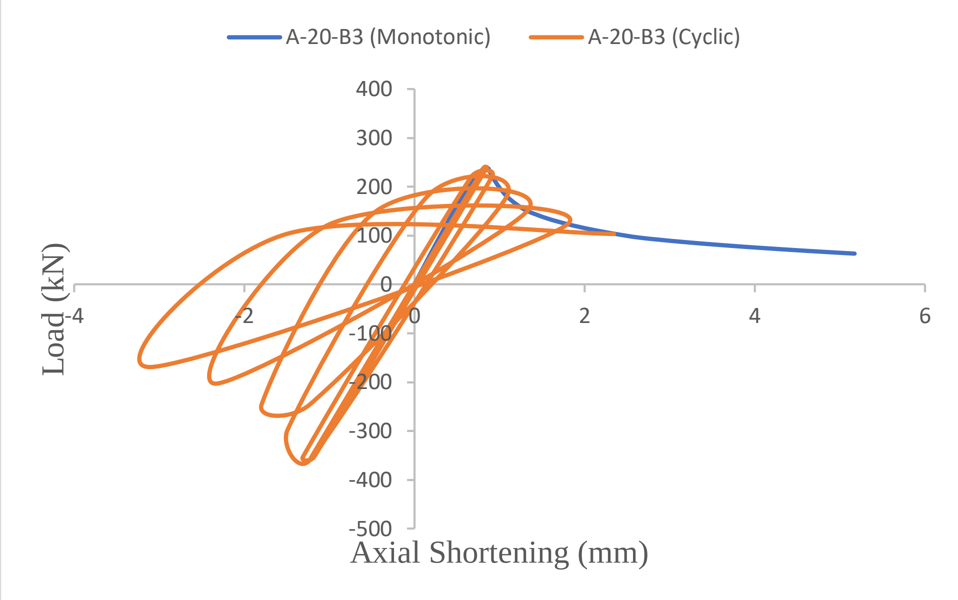

Figure 5 Monotonic and Cyclic Load-Axial Shortening Response of Specimen A-20-B3.

Discussion:

From the comparison of result it is found that, evaluating the resistance of a build-up battened column member as the sum of resistance of individual chords is not representative of the actual structural response of these member. The conservatively predicts the ultimate capacity of build-up battened column. Here the conservatism increases with increase member slenderness ratio. Equal angle sections are mainly failed due to local (L) buckling, sometimes due to distortional (D) or flexural (F) with local (L) buckling. For the slenderness ratio less than 70 all the specimen of channel section failed by combined local (L), distortional (D) and flexural (F) mode. For slenderness ratio greater than 70 of channel sections and hat sections for all slenderness ratio the specimens failed by combined distortional (D) and flexural (F) mode. But the predominate mode is distortional buckling also govern the strength. From the result obtained the following comparisons have been mode for equal angle, channel section with and without lip and hat section columns. The cyclic response approach unconservative predicts the strength of the build-up battened columns. The conservatism increases while increasing member slenderness ratio. By looking at figure 5 found that the cyclic response and FEM curve follows same trend. For slenderness ratio greater than 70 the rate of conservatism is more for channel section. The graph shows that the curve has a similar pattern. So, their behaviour will be similar irrespective of the cross section.

Conclusions:

From series of tests conducted on welded batten column made of equal angle section, channel sections with and without lip arrange in face-to-face and back-to-back fashion and hat section for varying slenderness ratio in this numerical study. The following conclusion based on the compression strength and axial cyclic response of the battened columns for pinned and fixed end condition are drawn:

- While increasing slenderness ratio after 40 the ultimate strength of batten columns is continuously decreases. In general, increase in length of batten column reduce load caring capacity across all sections.
- The ultimate strength of the member results of Finite element analysis and Axial cyclic response are close to 9%. In which results of pinned end were much closer than fixed end condition.
- The ultimate load caring capacity of fixed end condition for 20 slenderness ratio is 34% average higher than pinned end condition which constantly decrease up to 11% average higher side for 120 slenderness ratios.

- Equal angle section performs slightly better than channel sections were channel section gives more constant and closed value and prove more reliable than other sections across all length. Hat section shows higher load carrying capacity than other sections but when it comes to higher slenderness ratio hat section gives lower values than others.
- The load carrying capacity for the channel welded face-to-face as box section is higher than that of channel welded back-to-back up to slenderness ratio 80 after that back-to-back sections perform slightly better.
- The provision of lip increases the load carrying capacity almost twice for channel sections.
- The load versus axial shortening behaviour is initially linear in all the cases up to 75% of ultimate load irrespective of the cross-section of the specimen.

Reference:

1. Konstantinos E. Kalochairetis, Charis J. Gantes, “Numerical and analytical investigation of collapse loads of laced built-up columns”, Comput. Struct. **2011**, 89, 1166–1176. DOI: http://dx.doi.org/10.1016/j.compstruc.2010.10.018
2. Krishanu Roy, Tina Chui Huon Ting, Hieng Ho Lau, James B.P. Lim, “Nonlinear behaviour of back-to-back gapped built-up cold-formed steel channel sections under compression”, J. Constr. Steel Res. **2018**, 147, 257–276. DOI: https://doi.org/10.1016/j.jcsr.2018.04.007
3. David A. Padilla-Llano, Cristopher D. Moen, Matthew R. Eatherton, “Cyclic axial response and energy dissipation of cold-formed steel framing members”, Thin-Walled Struct. **2014**, 78, 95-107. DOI: http://dx.doi.org/10.1016/j.tws.2013.12.011
4. Iveta Georgieva, Luc Schueremans, Lincy Pyl, “Composed columns from cold-formed steel Z-profiles: Experiments and code-based predictions of the overall compression capacity”, Eng. Struct. **2012**, 37, 125–134. DOI: http://dx.doi.org/10.1016/j.engstruct.2011.12.017
5. Jun Ye, Iman Hajirasouliha, Jurgen Becque, Abolfazl Eslami, “Optimum design of cold-formed steel beams using Particle Swarm Optimisation method, J. Constr. Steel Res. **2016**, 122, 80–93. DOI: http://dx.doi.org/10.1016/j.jcsr.2016.02.014
6. P.B. Dinis, D. Camotim, “Cold-formed steel columns undergoing local–distortional coupling: Behaviour and direct strength prediction against interactive failure”, Comput. Struct. **2015**, 147, 181–208. DOI: http://dx.doi.org/10.1016/j.compstruc.2014.09.012
7. G Beulah Gnana Ananthi, S Vishuvardhan & G M Samuel Knight, “Experimental, theoretical and numerical study on thin walled steel single and compound channel section in axial compression”, Indian Jl. Of Engg. And Mat. Sci., Vol. 22, **2015**, pp 570–580. DOI: https://doi.org/10.1007/s42107-018-0096-2
8. Jun Yea, Iman Hajirasoulihaa, Jurgen Becquea, “Experimental investigation of local-flexural interactive buckling of coldformed steel channel columns”, Thin-Walled Struct. **2018**, 125, 245–258. DOI: https://doi.org/10.1016/j.tws.2018.01.020
9. K. C. Kalam Aswathy and M. V. Anil Kumar, “Unstiffened Elements as Limiting Case of Distortional Buckling of Partially Stiffened Elements”, J. Struct. Eng. **2020**, 146, 04020171. DOI: https://doi.org/10.1061/(ASCE)ST.1943-541X.0002712
10. M. Adil Dar, Dipti Ranjan Sahoo, Arvind K. Jain, “Influence of chord compactness and slenderness on axial compression behavior of built-up battened CFS columns”, J. Build. Eng. **2020**, 32, 101743. DOI: https://doi.org/10.1016/j.jobe.2020.101743
11. Soumia Kherbouche, Abdellatif Megnounif, “Numerical study and design of thin walled cold formed steel built-up open and closed section columns”, Eng. Struct. **2019**, 179, 670–682. DOI: https://doi.org/10.1016/j.engstruct.2018.10.069
12. P. Manikandan · N. Arun, “Behaviour of Partially Closed Stiffened Cold-Formed Steel Compression Member”, Arab. J. Sci. Eng. **2016**, 41, 3865–3875. DOI: http://doi.org/10.1007/s13369-015-2015-0
13. R.L. Madsen, N. Nakata, B.W. Schafer, “CFS-NEES Building Structural Design Narrative”, research report, RR01c, October **2011**. URL: http://jhir.library.jhu.edu/handle/1774.2/40584